Buckling load variability of cylindrical shells with stochastic imperfections

George Stefanou*, Vissarion Papadopoulos and Manolis Papadrakakis

Institute of Structural Analysis & Antiseismic Research,
National Technical University of Athens,
9, Iroon Polytechniou Str., Zografou Campus,
GR-15780 Athens, Greece
Email: stegesa@central.ntua.gr
Email: vpapado@central.ntua.gr
Email: mpapadra@central.ntua.gr
*Corresponding author

Abstract: In this paper, the effect of random initial geometric, material and thickness imperfections on the buckling load of isotropic cylindrical shells is investigated. To this purpose, a stochastic spatial variability of the elastic modulus as well as of the thickness of the shell is introduced in addition to the random initial geometric deviations of the shell structure from its perfect geometry. The modulus of elasticity and the shell thickness are described by two-dimensional univariate (2D-1V) homogeneous non-Gaussian translation stochastic fields. The initial geometric imperfections are described as a 2D-1V homogeneous Gaussian stochastic field. A numerical example is presented examining the influence of the non-Gaussian assumption on the variability of the buckling load. In addition, useful conclusions are derived concerning the effect of the various marginal probability density functions as well as of the spectral densities of the involved stochastic fields on the buckling behaviour of shells, as a result of a detailed sensitivity analysis.

Keywords: stochastic finite element; buckling load; random imperfections; non-Gaussian stochastic fields; spectral representation.

Reference to this paper should be made as follows: Stefanou, G., Papadopoulos, V. and Papadrakakis, M. (2011) 'Buckling load variability of cylindrical shells with stochastic imperfections', *Int. J. Reliability and Safety*, Vol. 5, No. 2, pp.191–208.

Biographical notes: George Stefanou graduated from the School of Civil Engineering of the National Technical University of Athens (NTUA). He received his post-graduate and PhD degrees in the field of Computational Stochastic Mechanics from NTUA. He is currently a Research Associate at the Institute of Structural Analysis and Antiseismic Research of NTUA. His research activity is mainly focused on the development and the application of computer methods for stochastic finite element analysis of real-world structures and on the efficient numerical simulation of stochastic processes and fields. He is member of the Scientific Committee of an IUTAM Symposium, reviewer for 24 scientific journals, one publishing company and 10 international conferences.

Vissarion Papadopoulos received his Civil Engineering degree and PhD in Stochastic Finite Element Method (SFEM) from the National Technical University of Athens (NTUA). In 2006, he joined the School of Civil Engineering of NTUA and specifically the Institute of Structural Analysis and Antiseismic Research, where he is currently a Lecturer and teaches five courses in the graduate and post-graduate levels, including structural analysis and design using SFEM (post-graduate course). His research activity is devoted to computational mechanics with emphasis on system uncertainties described by random fields.

Manolis Papadrakakis is a Professor of Structural Engineering at the School of Civil Engineering of the National Technical University of Athens. His research activity is focused on the development and the application of computer methods and technology to Simulation Based Engineering Science. He is Editor of the *International Journal of Computer Methods in Applied Mechanics and Engineering* (*CMAME*); Honorary Editor of the *International Journal of Computational Methods* (*IJCM*); President of the European Community on Computational Methods in Applied Sciences (ECCOMAS); Member of the editorial board of 16 international scientific journals and reviewer for 50 scientific journals.

1 Introduction

The buckling behaviour of shell structures is strongly influenced by their initial imperfections which occur during the manufacturing and construction stages. It was soon realised that the wide scatter in measured buckling loads of shell structures could only be approximated through numerical modelling taking into account the randomness of the imperfect geometries (Chryssanthopoulos and Poggi, 1995; Bielewicz and Górski, 2002; Schenk and Schuëller, 2003; Stull et al., 2008). In addition to the initial geometric imperfections, other sources of imperfections such as the variability of thickness, material properties, boundary conditions and misalignment of loading are also responsible for the reduction and scatter of the buckling load of shell structures (Palassopoulos, 1993; Morris, 1996; Li et al., 1997; Elishakoff, 2000; Arbocz and Starnes, 2002).

One of the first attempts to represent shape (radius and thickness) imperfections by spatially varying stochastic fields is that of Choi and Noh (2000). In that paper, the response variability of a reinforced concrete cooling tower shell due to shape imperfections is investigated. The variability of the random buckling loads of beams and plates with stochastically varying material and geometric properties is studied by Graham and Siragy (2001) using the concept of the variability response function. Tsouvalis et al. (2003) examined the effect of geometric imperfections and of boundary conditions on the buckling behaviour of composite cylinders under external hydrostatic pressure in a deterministic finite element framework. Papadopoulos and Papadrakakis (2004, 2005) computed the buckling load variability of cylindrical panels with geometric, material and thickness imperfections described by Gaussian stochastic fields. Papadopoulos and Iglesis (2007) further examined the effect of random boundary imperfections (simulated as a non-uniform random axial loading) on the buckling behaviour of isotropic thin-walled imperfect cylindrical shells. Schenk and Schuëller (2007) investigated the effect of random boundary and geometric imperfections on the critical load of isotropic

thin-walled cylindrical shells with rectangular cut-outs under axial compression. Onkar et al. (2007) presented a stochastic buckling analysis of laminated composite plates, with and without circular cut-outs, based on a first-order perturbation technique. The effect of uncertain material properties on the buckling strength of the laminated plates is studied taking into account the influence of variation in microlevel constituents on the effective macrolevel elastic properties.

An accurate prediction of the buckling behaviour of shells requires a realistic description of all uncertainties involved in the problem. Such a task is realisable only in the framework of a robust Stochastic Finite Element Method (SFEM) formulation that can efficiently and accurately handle the geometric as well as physical nonlinearities of shell-type structures (e.g. Choi and Noh, 2000; Graham and Siragy, 2001; Argyris et al., 2002b; Bielewicz and Górski, 2002; Schenk and Schuëller, 2003; Papadopoulos and Papadrakakis, 2004; Stefanou and Papadrakakis, 2004; Papadopoulos and Papadrakakis, 2005; Onkar et al., 2007; Papadopoulos and Iglesis, 2007; Schenk and Schuëller, 2007; Chang et al., 2008; Stull et al., 2008; Papadopoulos et al., 2009; Alibrandi et al., 2010).

Recent research efforts were mainly focused on the application of the SFEM to the buckling analysis of shell-type structures aiming at reducing the scatter of the computed buckling loads with respect to experimental results. The main difficulty in applying this methodology has been the lack of experimental data that would enable a proper quantification of the involved uncertain parameters. As a result, a sensitivity analysis was usually required with respect to various probabilistic characteristics describing the involved stochastic fields, such as standard deviation and spectral density, leading to the identification of 'worst case' scenarios with regard to the mean value and standard deviation of the predicted buckling loads. In these studies, a Gaussian assumption was always made for the corresponding marginal probability density functions (Choi and Noh, 2000; Graham and Siragy, 2001; Papadopoulos and Papadrakakis, 2004; Papadopoulos and Papadrakakis, 2005; Papadopoulos and Iglesis, 2007; Schenk and Schuëller, 2007; Chang et al., 2008).

In this paper, the effect of combined geometric, material and thickness variations on the buckling load of thin isotropic imperfect cylindrical shells is examined taking into account additional sensitivities due to various non-Gaussian assumptions. To this purpose, a non-Gaussian spatial variability of the elastic modulus as well as of the thickness of the shell is introduced in addition to the random initial geometric imperfections. The initial geometric imperfections are described as a two-dimensional univariate (2D-1V) homogeneous Gaussian stochastic field, which is simulated via the spectral representation method (Shinozuka and Deodatis, 1996). The modulus of elasticity and the shell thickness are described by 2D-1V uncorrelated homogeneous non-Gaussian stochastic fields using the spectral representation method in conjunction with the translation field theory (Grigoriu, 1984; Grigoriu, 1995; Deodatis and Micaletti, 2001; Lagaros et al., 2005; Bocchini and Deodatis, 2008).

The numerical example presented herewith examines the relative influence of the non-Gaussian assumption (a lognormal and three different beta distributions are used) on the variability of the buckling load, which is calculated by means of the Monte Carlo Simulation (MCS) method. For the determination of the limit load of the shell, a stochastic formulation of the geometrically nonlinear elastoplastic facet triangular shell element TRIC is implemented (Argyris et al., 1998; Argyris et al., 2002b). A shallow hinged isotropic cylindrical panel with a point load at the mid of its top surface is

selected as test example. This shell exhibits a limit point buckling with large pre-buckling deformation response. As a result of a detailed sensitivity analysis, useful conclusions are derived concerning the effect of the spectral characteristics of the geometric, material and thickness imperfections on the buckling behaviour of the shell structure.

2 Finite element formulation

The finite element simulation is performed with the triangular element TRIC, which is based on the natural mode method. The TRIC shear-deformable facet shell element is a reliable and cost-effective element suitable for linear and nonlinear analysis of thin and moderately thick isotropic as well as composite plate and shell structures (Argyris et al., 1998; Argyris et al., 2002a; Argyris et al., 2002b). The element has 18 degrees of freedom (6 per node) and hence 12 natural straining modes (Figure 1). Three natural axial strains and natural transverse shear strains are measured parallel to the edges of the triangle. The stiffness is contributed only by deformations and not by the associated rigid body motions. The natural stiffness matrix can be produced from the statement of variation of the strain energy with respect to the natural coordinates.

Figure 1 The multilayer TRIC shell element; coordinate systems

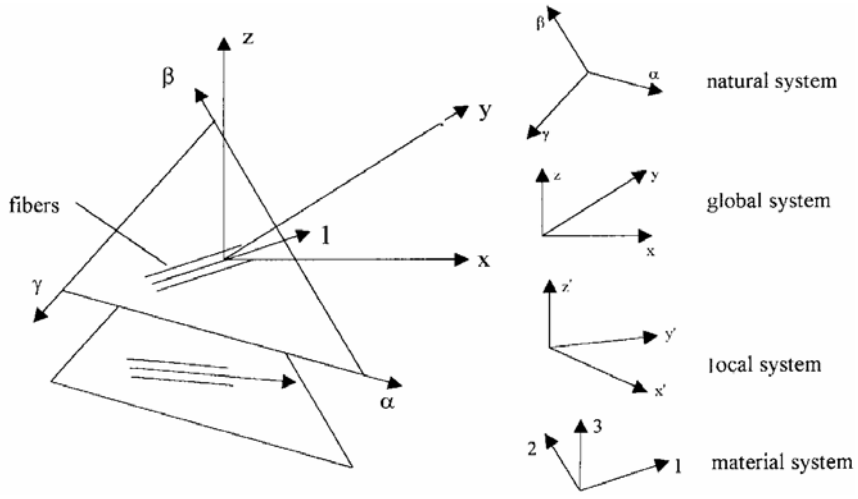

The geometric stiffness is based on large deflections but small strains and consists of two parts: a geometric stiffness matrix generated by the rigid-body movements of the element and a natural geometric stiffness matrix arising from the coupling between the axial forces and the symmetric bending modes (stiffening or softening effect). In order to form the geometric stiffness, small rigid-body rotational increments about the local Cartesian axes are considered:

$$d\rho_0^2 = \left[d\rho_{04} \quad d\rho_{05} \quad d\rho_{06} \right]^T \tag{1}$$

These rigid-body rotational increments correspond to nodal Cartesian moments dM_0 along the same axes. Using the fact that the resultants of all forces produced by rigid-body motion must vanish, the following expression is derived for dM_0:

$$\underset{(3x1)}{dM_0} = \underset{(3x3)}{\bar{k}_{GR}}\ \underset{(3x1)}{d\rho_0^2} \tag{2}$$

where $\bar{k}_{GR}$ is the local rigid-body rotational geometric stiffness. As can be seen in paper by Argyris et al. (1998), $\bar{k}_{GR}$ has a simple analytical form. Only the middle plane axial natural forces, which fully represent the pre-stress state within the material, are included in the stiffness matrix. The natural geometric stiffness matrix arising from the coupling between the axial forces and the symmetric bending modes is of diagonal form:

$$k_{NG} = \frac{1}{12}\left[\,.\quad .\quad .\quad P_\alpha\quad .\quad P_\beta\quad .\quad P_\gamma\quad .\quad .\quad .\quad .\right] \tag{3}$$

where P_α, P_β, P_γ are the middle plane axial natural forces. The natural geometric stiffness is first transformed to the local and ultimately to the global coordinate system.

In the case of material nonlinearity (Argyris et al., 2002a), the elastoplastic constitutive matrix κ_{ct}^{el} is established by obtaining the relation between the natural strain and stress increments for each layer 'r' within a given load step:

$$d\sigma_c^r = \left[\kappa_{ct}^{el} - \frac{1}{H + s_N^T \kappa_{ct}^{el} s_N}(\kappa_{ct}^{el} s_N)(\kappa_{ct}^{el} s_N)^T\right]^r d\gamma_t^r \tag{4}$$

where H is the hardening parameter, s_N is obtained by the normality flow rule as

$$s_N = \frac{\partial F}{\partial \sigma_c} = \left[\frac{\partial F}{\partial \sigma_{c\alpha}}\quad \frac{\partial F}{\partial \sigma_{c\beta}}\quad \frac{\partial F}{\partial \sigma_{c\gamma}}\right]^T \tag{5}$$

and the expression in brackets corresponds to the elastoplastic material stiffness matrix $\kappa_{ct}^{el\text{-}pl}$ valid for every layer 'r':

$$[\kappa_{ct}^{el-pl}]^r = \left[\kappa_{ct}^{el} - \frac{1}{H + s_N^T \kappa_{ct}^{el} s_N}(\kappa_{ct}^{el} s_N)(\kappa_{ct}^{el} s_N)^T\right]^r \tag{6}$$

The natural elastoplastic stiffness of the element is finally obtained by summing up the natural elastoplastic stiffnesses of the element layers.

3 Stochastic initial geometric imperfections

The imperfect geometry of shell structures is usually represented as a two-dimensional univariate (2D-1V) stochastic field. The statistical properties of this stochastic field modelling the initial geometric imperfections can be based either on experimental measurements or on an assumed variation in cases where no experimental results are available. Previous work on the subject (Schenk and Schuëller, 2003; Papadopoulos and

Papadrakakis, 2005) has been mainly focused on the buckling behaviour of axially compressed cylinders for which a data bank of experimentally measured initial imperfections is available (Arbocz and Abramovich, 1979). In this early work, the stochastic description of the geometric imperfections was based on a statistical analysis of the experimentally measured imperfections. The obtained results clearly demonstrated that the stochastic field of the initial geometric imperfections is non-homogeneous, while the Gaussian distribution fits well the experimental data.

In the present paper, initial geometric imperfections are modelled as a homogeneous two-dimensional Gaussian stochastic field. The assumption of homogeneity, although not generally applicable for the description of initial imperfections of shells, is adopted in this study and elsewhere (Papadopoulos and Papadrakakis, 2004; Papadopoulos and Papadrakakis, 2005) for simplicity as well as due to the fact that there are no experimental data available for the particular type of cylindrical panel used as test example. For this reason, a parametric study was performed by Papadopoulos and Papadrakakis (2004), with respect to the correlation lengths of the stochastic field in both x and y directions. The outcome of the parametric study revealed the 'worst' imperfection mode of the shell.

More specifically, the radius of the cylindrical shell is assumed to be a 2D-1V homogeneous stochastic field, which can be expressed as follows:

$$r(x,y) = r_0 + g(x,y) \cdot h \tag{7}$$

where r(x,y) is the varying initial radius at each point of the structure, r_0 is the radius of the perfect geometry, g(x,y) is a zero-mean homogeneous Gaussian stochastic field and h is the height of the cylindrical panel. In the present work, the amplitude of the imperfections, which is controlled by the standard deviation of the stochastic field, is selected to be a percentage of the height 'h' of the cylindrical panel. The coordinates x and y are the global Cartesian coordinates of the unfolded panel.

4 Stochastic finite element analysis

The modulus of elasticity and the thickness of the shell are also considered in the present study as 'imperfections', due to their spatial variability. These parameters are described by two uncorrelated 2D-1V homogeneous non-Gaussian stochastic fields:

$$E(x,y) = E_0 \left[1 + f_1(x,y)\right] \tag{8}$$

$$t(x,y) = t_0 \left[1 + f_2(x,y)\right] \tag{9}$$

where E_0 is the mean value of the elastic modulus, t_0 is the mean thickness of the structure and $f_1(x,y)$, $f_2(x,y)$ are two zero-mean non-Gaussian homogeneous stochastic fields corresponding to the variability of the modulus of elasticity and the thickness of the shell, respectively.

The stochastic stiffness matrix of the shell element is derived using the midpoint method, i.e. one integration point at the centroid of each finite element is used for the computation of the stiffness matrix.

5 Simulation of material and thickness imperfections using non-Gaussian translation fields

In this work, a non-Gaussian assumption is made for the distribution of material and thickness imperfections. This choice is in accordance to the fact that several quantities arising in practical engineering problems (e.g. material and geometric properties of structural systems) are found to exhibit non-Gaussian probabilistic characteristics. In addition, the non-Gaussian assumption permits to efficiently treat the case of large input variability without violating the physical constraints of the material and geometric properties.

Since all the joint multi-dimensional density functions are needed to fully characterise a non-Gaussian stochastic field, much of the existing research has focused on a more realistic way of defining a non-Gaussian sample function as a simple transformation of some underlying Gaussian field with known second-order statistics. Thus, if g(**x**) is a homogeneous zero-mean Gaussian field with unit variance and spectral density function (SDF) $S_{gg}(\boldsymbol{\kappa})$ (or equivalently autocorrelation function $R_{gg}(\boldsymbol{\xi})$), a homogeneous non-Gaussian stochastic field f(**x**) with power spectrum $S_{ff}^{T}(\boldsymbol{\kappa})$ can be defined as:

$$\mathrm{f}(\mathbf{x}) = F^{-1} \cdot \Phi[\mathrm{g}(\mathbf{x})] \tag{10}$$

where Φ is the standard Gaussian cumulative distribution function and F is the non-Gaussian marginal cumulative distribution function of f(**x**). The transform $F^{-1} \cdot \Phi$ is a memory-less translation since the value of f(**x**) at an arbitrary point **x** depends only on the value of g(**x**) at the same point and the resulting non-Gaussian field is called a translation field (Grigoriu, 1984).

Translation fields have a number of useful properties such as the analytical calculation of crossing rates and extreme value distributions (Grigoriu, 1995). They also have some shortcomings, the most important of which from a practical point of view is the possible incompatibility between their marginal distribution F and correlation structure $S_{ff}^{T}(\boldsymbol{\kappa})$ (Deodatis and Micaletti, 2001). Since experimental data can lead to a theoretically incompatible pair of F and $S_{ff}^{T}(\boldsymbol{\kappa})$, iterative algorithms have been recently developed, which extend the translation field concept and lead to the generation of non-Gaussian fields having the prescribed characteristics (Deodatis and Micaletti, 2001; Lagaros et al., 2005; Bocchini and Deodatis, 2008).

In the present work, non-Gaussian translation sample functions obtained from equation (10) are used, since there are no experimental data imposing a specific pair of $F - S_{ff}^{T}(\boldsymbol{\kappa})$. The SDF $S_{gg}(\boldsymbol{\kappa})$ of the underlying Gaussian field used in the numerical example is assumed to correspond to an autocorrelation function of square exponential type and is given by:

$$S_{gg}(\kappa_1, \kappa_2) = \sigma_g^2 \frac{\mathrm{b}_1 \mathrm{b}_2}{4\pi} \exp\left[-\frac{1}{4}(\mathrm{b}_1^2 \kappa_1^2 + \mathrm{b}_2^2 \kappa_2^2) \right] \tag{11}$$

where σ_g denotes the standard deviation of the stochastic field and $\mathrm{b}_1, \mathrm{b}_2$ denote the parameters that influence the shape of the spectrum, which are proportional to the correlation lengths of the stochastic field along the x, y axes, respectively. The SDF of the translation field obtained from equation (10) will slightly differ from $S_{gg}(\boldsymbol{\kappa})$ as shown by Papadopoulos et al. (2009).

6 Numerical example

A test example is presented in this section in order to demonstrate the applicability as well as the efficiency of the proposed methodology. It is a shallow hinged isotropic cylindrical panel shown in Figure 2. This example is chosen because it exhibits a highly nonlinear behaviour with considerable influence of the physical nonlinearities on the overall structural response. The loading as well as the geometric and material properties of the perfect shell are also shown in Figure 2. The cylindrical panel is discretised with a 21 × 21 mesh of 800 TRIC shell elements. The material is considered to be elastic-perfectly plastic. The curve edge nodes of the panel are assumed to be free in all directions while the nodes along the sides are hinged (fixed against translation).

Figure 2 Geometry, material data and finite element mesh used in the discretisation of the cylindrical panel

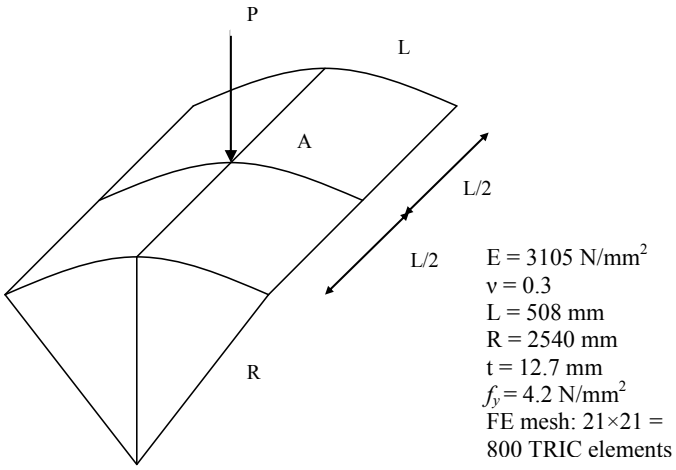

The geometrically nonlinear elastic as well as elastoplastic response of point A of the perfect cylinder with respect to the applied vertical load P is shown in Figure 3. The load-displacement curve has been obtained using a path-following strategy based on the arc-length method, described in detail by Argyris et al. (1998) where a mesh convergence study for this particular example is also presented. For the discretisation of the stochastic fields, the same mesh used for the finite element analysis is implemented since it is a fraction of the correlation length parameters adopted in this example. Thus, it is considered dense enough for the accurate representation of the fluctuations of the stochastic fields (Li and Der Kiureghian, 1993). The ultimate load of the perfect configuration is found to be $P_u = 2205$ N for the elastic and $P_u = 1240$ N for the elastoplastic shell.

6.1 Initial geometric imperfections

2D stochastic geometric imperfections are first introduced to the model in order to investigate their effect on the buckling load of the panel. The mean thickness of the shell is considered to be equal to the height 'h' at the apex of the cylinder, i.e. $t_0 = 12.7$ mm. The standard deviation σ_g of the Gaussian stochastic field describing the imperfections is

assumed to be 20%. Since no experimental data of initial imperfections are available for this specific type of structure, a parametric study was performed by Papadopoulos and Papadrakakis (2004) with respect to the correlation lengths of the stochastic field in both x, y directions using a sample size N_{SAMP} = 100. This sample size is sufficient for the accurate computation of the first two statistical moments of the buckling load. It was assumed that the correlation lengths in both directions are equal ($b_1 = b_2 = b$) since there is no evidence of any specific manufacturing procedure or boundary conditions that would indicate a different assumption. The outcome of the parametric study was the evaluation of the 'worst' imperfection mode of the shell (Figure 4), which led to the estimation of the lower bound of the buckling load of the shell with and without physical nonlinearities (900 and 1250 N, respectively). A non-Gaussian assumption for the geometric imperfections (with the same standard deviation σ_f = 20%) resulted in practically the same 'worst' imperfection mode and lower bounds of the buckling load of the shell.

Figure 3 Central load – displacement curve of the perfect cylindrical panel for t = 12.7 mm (see online version for colours)

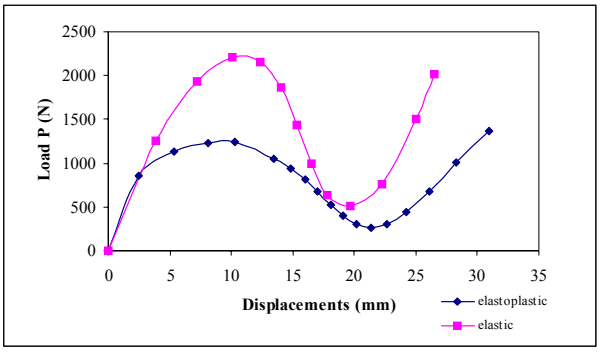

Figure 4 Sample function of 2D initial imperfection shapes of the cylindrical panel for σ_g = 20% and $b_1 = b_2$ = 250 mm ('worst imperfection mode') (see online version for colours)

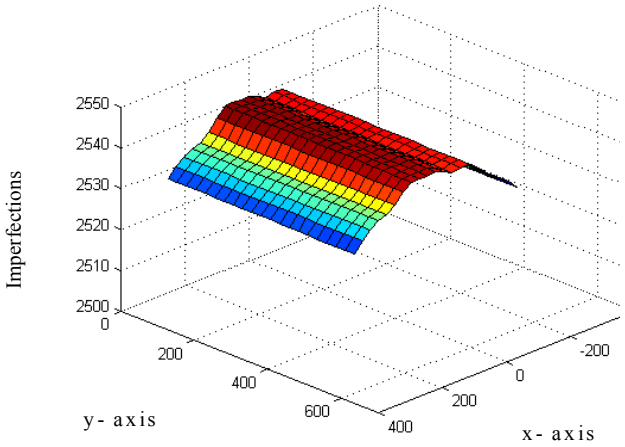

6.2 Material and thickness imperfections

Sensitivity analyses for a Gaussian variation of the Young modulus and shell thickness have been performed by Papadopoulos and Papadrakakis (2004). As explained in Section 5, a non-Gaussian assumption is made in this work for the distribution of the two uncertain parameters. In Figures 7 and 8, the mean value and the coefficient of variation (Cov) of the buckling load are plotted against the correlation length parameter 'b' of the underlying Gaussian field for a non-Gaussian stochastic variation of the Young modulus and thickness of the structure. A lognormal and three different cases of beta distribution with zero mean and σ_f = 10% are assumed to describe the variation of the two uncertain properties. The parameters of the aforementioned distributions are presented in Table 1. Sample functions of the corresponding stochastic fields are generated for each value of 'b' using equations (10), (11) and the spectral representation method (Shinozuka and Deodatis, 1996) for the simulation of the underlying Gaussian fields. Monte Carlo Simulation (MCS) with sample size N_{SAMP} = 100 is again used for the calculation of the buckling load variability. Statistical convergence is achieved within this number of simulations for the first two moments of P_u, as shown in Figure 5a. Only the lognormal distribution is examined in Figures 5, 7 and 8. The three beta distributions lead to similar results.

Figure 5 Mean value and coefficient of variation (Cov) of the ultimate load P_u as a function of the number of simulations for 2D variation of (a) the modulus of elasticity, and (b) combined geometric, material and thickness imperfections (lognormal distribution – elastic shell)

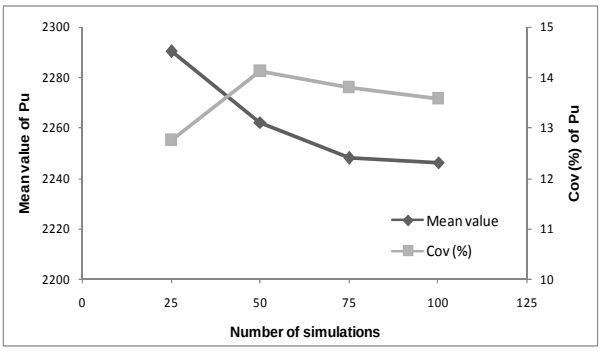

(a)

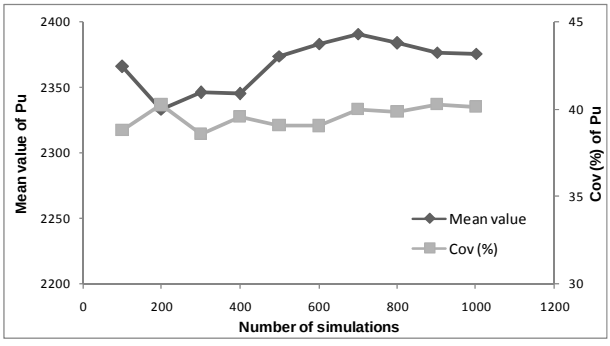

(b)

Figure 6 Mean value and coefficient of variation (Cov) of the ultimate load P_u as a function of the correlation length parameter b for 2D variation of (a) the modulus of elasticity, and (b) the thickness (Gaussian distribution, σ_f= 10% – elastic shell) (see online version for colours)

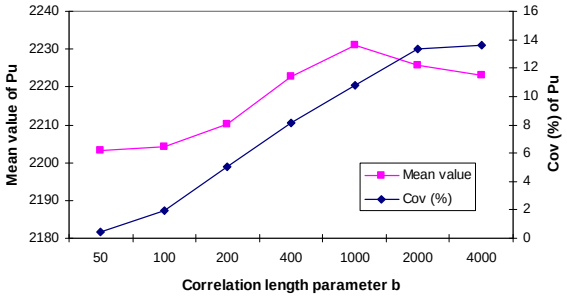

(a)

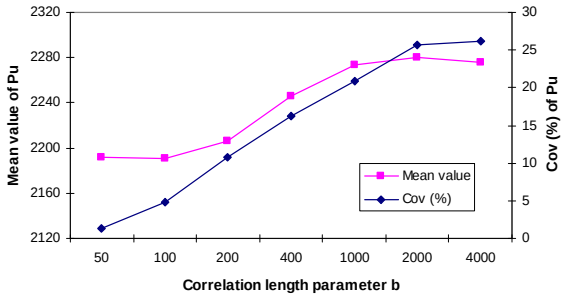

(b)

Figure 7 Mean value and coefficient of variation (Cov) of the ultimate load P_u as a function of the correlation length parameter b for 2D variation of (a) the modulus of elasticity, and (b) the thickness (lognormal distribution, σ_f= 10% – elastic shell) (see online version for colours)

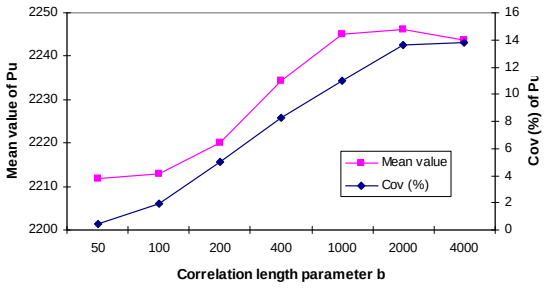

(a)

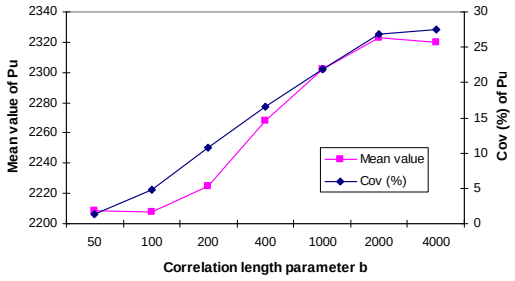

(b)

Figure 8 Mean value and coefficient of variation (Cov) of the ultimate load P_u as a function of the correlation length parameter b for 2D variation of (a) the modulus of elasticity, and (b) the thickness (lognormal distribution, σ_f = 10% – elastoplastic shell) (see online version for colours)

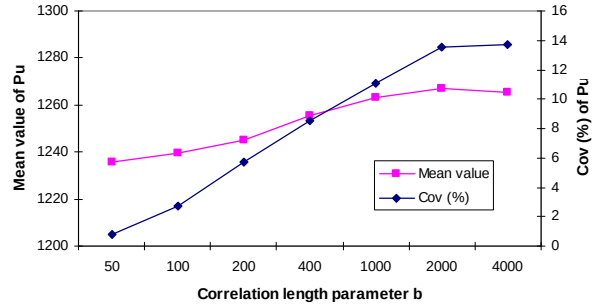

(a)

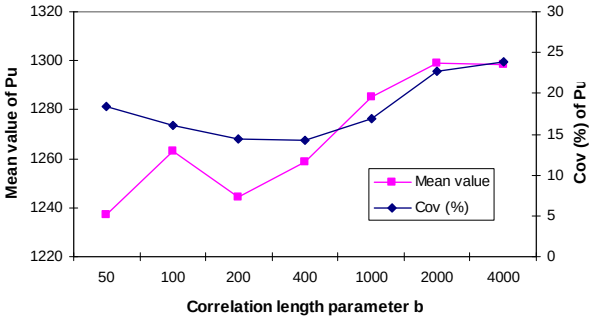

(b)

Table 1 Range of definition and shape parameters of lognormal and beta distributions

	Lower bound	*Upper bound*	*Shape parameters*	
Lognormal	–1	+∞	–	–
Beta – Case 1	–0.5	0.5	p =12	q = 12
U-beta – Case 2	–0.16	0.16	p = 0.8	q = 0.8
L-beta – Case 3	–0.13	0.26	p = 0.8	q = 1.6

As can be seen in Figures 7 and 8 which is also observed in the case of Gaussian material and thickness variability (Figure 6), the 'worst' imperfection mode corresponds to a correlation length parameter $b_1 = b_2 = 2000$ mm (for both cases of geometric and physical nonlinearity), which is markedly different from $b_1 = b_2 = 250$ mm, corresponding to the 'worst' imperfection mode for initial geometric imperfections (Figure 4). For the elastic shell (Figures 6 and 7), the Cov of the buckling loads reaches a maximum value of approximately 13% (=1.3σ_f) for the material imperfections, while the maximum Cov for the spatial variation of the thickness is 26% (=2.6σ_f). Slightly smaller values of Cov are observed for the elastoplastic response of the shell (Figure 8). The results indicate a large magnification of uncertainty, which is even more pronounced for the case of combined geometric, material and thickness imperfections examined below. The mean value of the

buckling load is almost the same with the buckling load of the perfect shell for the Young modulus variation (Figures 6a–8a) while, in the case of thickness variation, it is somehow higher especially for large values of 'b' (Figures 6b–8b).

It is worth noting that the selection of the 'worst' imperfection mode in all cases is based on the maximum value of Cov and the minimum value of the lowest buckling load which occur at $b_1 = b_2 = 2000$ mm for both material and thickness variability. The term 'lowest buckling load' (P_{low}) means that the probability p of not exceeding P_{low} is equal to $1/N_{SAMP}$ with a corresponding confidence level. Sample functions of the stochastic fields related to the smallest buckling load for Young modulus and thickness variation considered as stand-alone cases are shown in Figure 9.

Figure 9 Sample functions of the stochastic fields leading to the smallest buckling load for (a) Young modulus and (b) thickness variation considered as stand-alone cases (lognormal distribution – elastic shell, L_x, L_y are the number of points in the x- and y-axes, respectively) (see online version for colours)

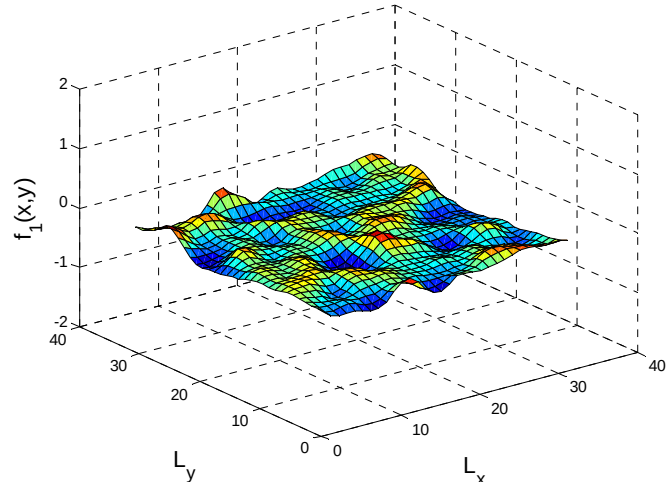

(a)

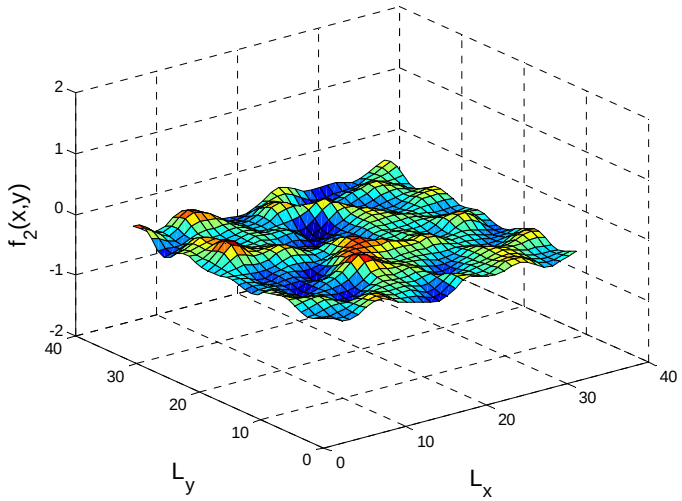

(b)

6.3 Combined geometric, material and thickness imperfections

All the above imperfections are now combined and introduced simultaneously to the model. For this purpose, the 'worst' imperfection modes and the corresponding correlation length parameters from the previously studied cases are combined. These values are $b_1 = b_2 = 250$ mm for the initial geometric imperfections ($\sigma_g = 20\%$) and $b_1 = b_2 = 2000$ mm for the variation of the modulus of elasticity and the thickness of the shell ($\sigma_f = 10\%$). For the combined imperfections, MCS is performed using a sample size $N_{SAMP} = 1000$, as opposed to $N_{SAMP} = 100$ used in the previous cases, since a larger sample size is required for the accurate prediction of the lowest buckling load of the panel. Statistical convergence is achieved within this number of simulations for the first two moments of P_u, as shown in Figure 5b.

Figure 10 presents the histograms of the buckling loads for the combined imperfections case, with and without physical nonlinearities. The first three statistical moments of P_u along with the lowest buckling loads observed in all the distribution cases considered, are summarised in Table 2. As can be seen in Figure 10 and in Table 2, the first two statistical moments of the buckling load seem to be independent from the marginal probability density function of the input parameters. This can be attributed to the fact that the initial geometric imperfections predominate due to the assumed high degree of variability ($\sigma_g = 20\%$). For all the distributions examined, the mean value of the buckling loads is around 2300 N for the elastic shell and 1300 N for the elastoplastic, which are a little bit higher than the respective buckling loads of the perfect shell. For the elastic shell, the Cov of P_u is around 40%, which is twice the value of Cov of geometric imperfections ($\sigma_g = 20\%$) and four times the value of Cov of material and thickness variation ($\sigma_f = 10\%$). In the elastoplastic case, the Cov of P_u is around 30%, which is 1.5 times the value of Cov of geometric imperfections and three times the value of Cov of material and thickness variation. However, the shape of the buckling load distribution is markedly different in each case, an observation that is confirmed by the different values of skewness given in Table 2. The lowest buckling loads are computed at 486 N in the elastic case (beta distribution) and 496 N in the elastoplastic case (normal distribution). It is worth noting that these values represent only the 22% and 40% of the buckling load of the perfect shells which are 2205 and 1240 N, respectively.

Table 2 Mean value, Cov, skewness and lowest values of P_u for different marginal probability density functions of Young modulus and thickness

		Mean value	*Cov (%)*	*Skewness*	*Lowest P_u*
Elastic shell	Gaussian	2336	40	0.87	501
	Lognormal	2375	40	0.99	565
	Beta	2324	39	0.77	486
	U-shaped beta	2308	37	0.61	717
	L-shaped beta	2347	39	0.95	792
Elastoplastic shell	Gaussian	1296	30	0.73	496
	Lognormal	1317	30	0.94	503
	Beta	1295	30	0.70	521
	U-shaped beta	1292	29	0.50	598
	L-shaped beta	1299	31	0.96	637

Figure 10 Histograms of the buckling load P_u for 2D variation of combined geometric, material and thickness imperfections: (a) Gaussian, (b) lognormal, (c) beta, (d) U-shaped beta and (e) L-shaped beta distribution of the material and thickness imperfections (see online version for colours)

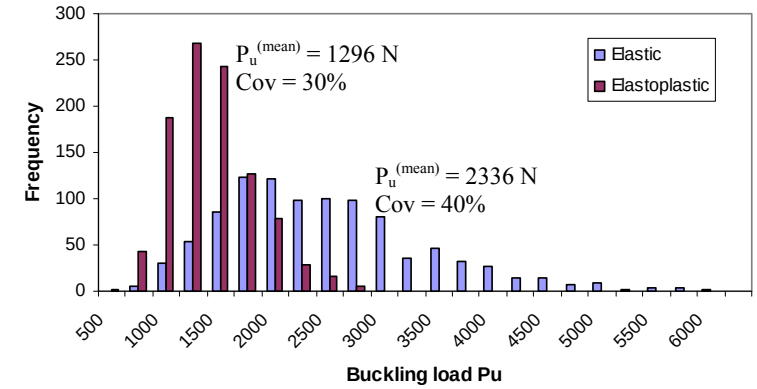

(a)

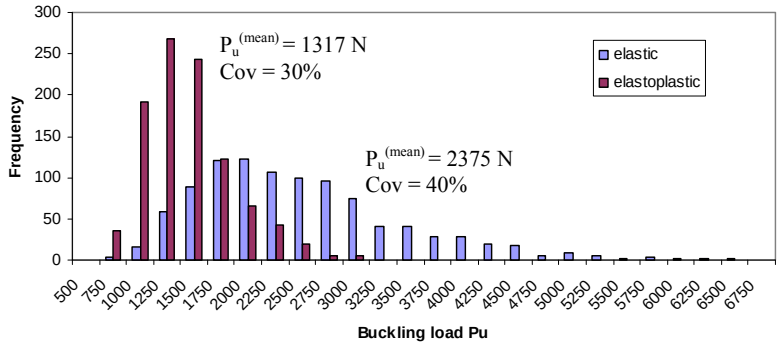

(b)

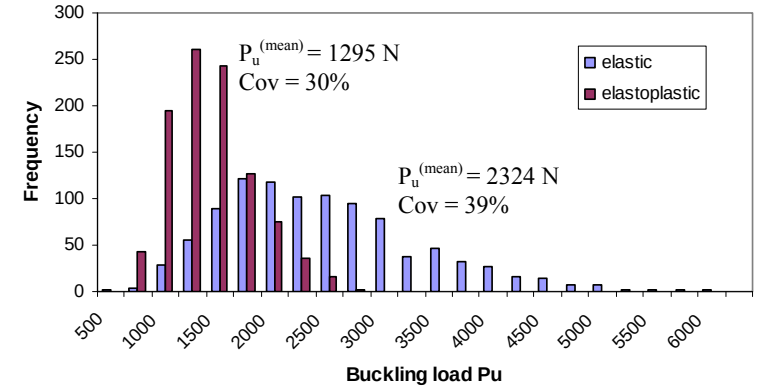

(c)

Figure 10 Histograms of the buckling load P_u for 2D variation of combined geometric, material and thickness imperfections: (a) Gaussian, (b) lognormal, (c) beta, (d) U-shaped beta and (e) L-shaped beta distribution of the material and thickness imperfections (see online version for colours) (continued)

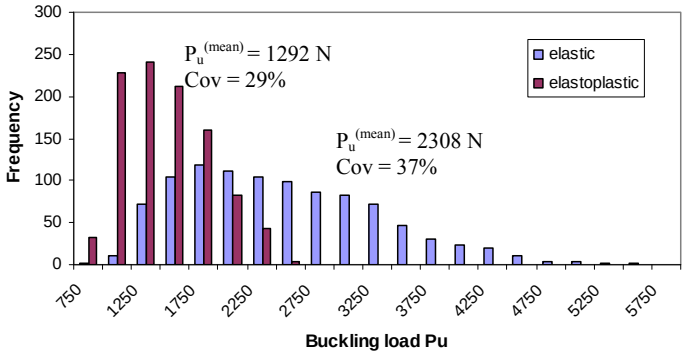

(d)

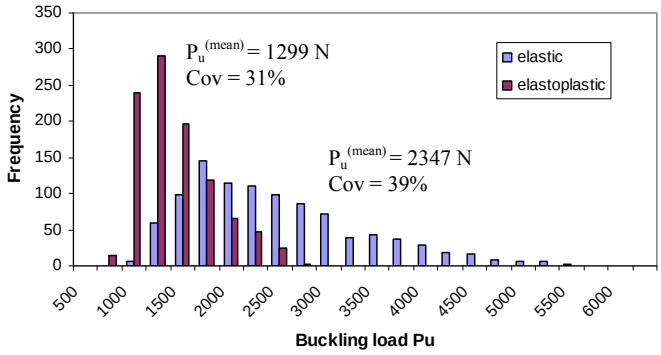

(e)

7 Conclusions

In this paper, the buckling load variability of isotropic cylindrical shells with random initial imperfections has been investigated. The modulus of elasticity and the shell thickness were described by uncorrelated homogeneous non-Gaussian translation fields. A detailed sensitivity analysis with respect to various marginal probability density functions and spectral characteristics of the material and thickness imperfections has been performed. As a result of this analysis, the first two statistical moments of the buckling load seemed to be independent from the marginal probability density function of the input parameters. However, the shape of the buckling load distribution was markedly different in each case. A large magnification of uncertainty has been observed in the buckling load variability, especially for the case of combined geometric, material and thickness imperfections. In that case, the Cov of the ultimate load has been found 1.5–2 times higher than the Cov of geometric imperfections and 3–4 times higher than the Cov of material and thickness imperfections. In addition, the lowest buckling loads

were found to represent only the 22% and 40% of the buckling load of the perfect elastic and elastoplastic shell, respectively. These observations underline the importance of realistic uncertainty quantification in shell buckling problems and can serve as guidelines for the robust design of imperfect shell structures.

References

Alibrandi, U., Impollonia, N. and Ricciardi, G. (2010) 'Probabilistic eigenvalue buckling analysis solved through the ratio of polynomial response surface', *Computer Methods in Applied Mechanics and Engineering*, Vol. 199, pp.450–464.

Arbocz, J. and Abramovich, H. (1979) *The initial imperfection data bank at the Delft University of Technology, Part 1*, Report LR-290, Department of Aerospace Engineering, Delft University of Technology.

Arbocz, J. and Starnes, J.H., Jr. (2002) 'Future directions and challenges in shell stability analysis', *Thin-Walled Structures*, Vol. 40, pp.729–754.

Argyris, J., Tenek, L., Papadrakakis, M. and Apostolopoulou, C. (1998) 'Post-buckling performance of the TRIC natural mode triangular element for isotropic and laminated composite shells', *Computer Methods in Applied Mechanics and Engineering*, Vol. 166, pp.211–231.

Argyris, J., Papadrakakis, M. and Karapitta, L. (2002a) 'Elastoplastic analysis of shells with the triangular element TRIC', *Computer Methods in Applied Mechanics and Engineering*, Vol. 191, pp.3613–3637.

Argyris, J., Papadrakakis, M. and Stefanou, G. (2002b) 'Stochastic finite element analysis of shells', *Computer Methods in Applied Mechanics and Engineering*, Vol. 191, pp.4781–4804.

Bielewicz, E. and Górski, J. (2002) 'Shells with random geometric imperfections: simulation-based approach', *International Journal of Non-Linear Mechanics*, Vol. 37, pp.777–784.

Bocchini, P. and Deodatis, G. (2008) 'Critical review and latest developments of a class of simulation algorithms for strongly non-Gaussian random fields', *Probabilistic Engineering Mechanics*, Vol. 23, pp.393–407.

Chang, T-P., Liu, M-F. and Chang, H-C. (2008) 'Finite element analysis of nonlinear shell structures with uncertain material property', *Thin-Walled Structures*, Vol. 46, pp.1055–1065.

Choi, C.K. and Noh, H.C. (2000) 'Stochastic analysis of shape imperfections in RC cooling tower shells', *Journal of Structural Engineering*, Vol. 126, pp.417–423.

Chryssanthopoulos, M.K. and Poggi, C. (1995) 'Stochastic imperfection modelling in shell buckling studies', *Thin-Walled Structures*, Vol. 23, pp.179–200.

Deodatis, G. and Micaletti, R.C. (2001) 'Simulation of highly skewed non-Gaussian stochastic processes', *Journal of Engineering Mechanics (ASCE)*, Vol. 127, pp.1284–1295.

Elishakoff, I. (2000) 'Uncertain buckling: its past, present and future', *International Journal of Solids and Structures*, Vol. 37, pp.6869–6889.

Graham, L.L. and Siragy, E.F. (2001) 'Stochastic finite element analysis for elastic buckling of stiffened panels', *Journal of Engineering Mechanics (ASCE)*, Vol. 127, pp.91–97.

Grigoriu, M. (1984) 'Crossings of non-Gaussian translation processes', *Journal of Engineering Mechanics (ASCE)*, Vol. 110, pp.610–620.

Grigoriu, M. (1995) *Applied non-Gaussian Processes*, Prentice-Hall, Englewood Cliffs, NJ.

Lagaros, N.D., Stefanou, G. and Papadrakakis, M. (2005) 'An enhanced hybrid method for the simulation of highly skewed non-Gaussian stochastic fields', *Computer Methods in Applied Mechanics and Engineering*, Vol. 194, pp.4824–4844.

Li, C-C. and Der Kiureghian, A. (1993) 'Optimal discretization of random fields', *Journal of Engineering Mechanics (ASCE)*, Vol. 119, pp.1136–1154.

Li, Y.W., Elishakoff, I., Starnes, J.H., Jr. and Bushnell, D. (1997) 'Effect of the thickness variation and initial imperfection on buckling of composite shells: asymptotic analysis and numerical results by BOSOR4 and PANDA2', *International Journal of Solids and Structures*, Vol. 34, pp.3755–3767.

Morris, N.F. (1996) 'Shell stability: the long road from theory to practice', *Engineering Structures*, Vol. 18, pp.801–806.

Onkar, A.K., Upadhyay, C.S. and Yadav, D. (2007) 'Stochastic finite element buckling analysis of laminated plates with circular cut-out under uniaxial compression', *Journal of Applied Mechanics (ASME)*, Vol. 74, pp.798–809.

Palassopoulos, G.V. (1993) 'New approach to buckling of imperfection-sensitive structures', *Journal of Engineering Mechanics (ASCE)*, Vol. 119, pp.850–869.

Papadopoulos, V. and Iglesis, P. (2007) 'The effect of non-uniformity of axial loading on the buckling behavior of shells with random imperfections', *International Journal of Solids and Structures*, Vol. 44, pp.6299–6317.

Papadopoulos, V. and Papadrakakis, M. (2004) 'Finite element analysis of cylindrical panels with random initial imperfections', *Journal of Engineering Mechanics (ASCE)*, Vol. 130, pp.867–876.

Papadopoulos, V. and Papadrakakis, M. (2005) 'The effect of material and thickness variability on the buckling load of shells with random initial imperfections', *Computer Methods in Applied Mechanics and Engineering*, Vol. 194, pp.1405–1426.

Papadopoulos, V., Stefanou, G. and Papadrakakis, M. (2009) 'Buckling analysis of imperfect shells with stochastic non-Gaussian material and thickness properties', *International Journal of Solids and Structures*, Vol. 46, pp.2800–2808.

Schenk, C.A. and Schuëller, G.I. (2003) 'Buckling analysis of cylindrical shells with random geometric imperfections', *International Journal of Non-Linear Mechanics*, Vol. 38, pp.1119–1132.

Schenk, C.A. and Schuëller, G.I. (2007) 'Buckling analysis of cylindrical shells with cut-outs including random boundary and geometric imperfections', *Computer Methods in Applied Mechanics and Engineering*, Vol. 196, pp.3424–3434.

Shinozuka, M. and Deodatis, G. (1996) 'Simulation of multi-dimensional Gaussian stochastic fields by spectral representation', *Applied Mechanics Reviews (ASME)*, Vol. 49, pp.29–53.

Stefanou, G. and Papadrakakis, M. (2004) 'Stochastic finite element analysis of shells with combined random material and geometric properties', *Computer Methods in Applied Mechanics and Engineering*, Vol. 193, pp.139–160.

Stull, C.J., Earls, C.J. and Aquino, W. (2008) 'A posteriori initial imperfection identification in shell buckling problems', *Computer Methods in Applied Mechanics and Engineering*, Vol. 198, pp.260–268.

Tsouvalis, N.G., Zafeiratou, A.A. and Papazoglou, V.J. (2003) 'The effect of geometric imperfections on the buckling behavior of composite laminated cylinders under external hydrostatic pressure', *Composites Part B: Engineering*, Vol. 34, pp.217–226.